THE AMERICAN SOCIETY OF MECHANICAL ENGINEERS
345 E. 47th St., New York, N.Y. 10017

94-GT-462

THE MODEL V84.3 SHOT TESTS: COMPRESSOR FLOW FIELD MEASUREMENTS AND EVALUATION

M. Janssen, R. Mönig, and J. Seume
KWU Group
Gas Turbine Technology
Siemens AG,
Mülheim, Germany

H. Hönen, R. Lösch-Schloms, and H. E. Gallus
Institut für Strahlantriebe und Turboarbeitsmaschinen
Rheinisch Westfälische Technische Hochschule
Aachen, Germany

ABSTRACT

Detailed experimental investigations were carried out at the Siemens test-facility in Berlin to validate and develop further the compressor design of the Model V84.3 gas turbine and to generate a comprehensive data base for the verification of the flow calculation programs. The test facility enables Siemens to confirm the design with regard to performance and reliability in the full scale machine under full load and off-design condition.

Various measuring techniques well established in the laboratory were applied to the full scale compressor to examine the flow field. Along with rather conventional 5-hole probes for measuring the flow field in the core region, miniaturized 3-hole probes were developed at the Turbomachinery Laboratory of the Technical University of Aachen, tested and finally used for the measurements of endwall boundary layer profiles and their development throughout the compressor. In addition to the probe measurements, wall static-pressure measurements, as well as probed vane measurements, were carried out.

The paper briefly describes the test facility, the compressor under investigation, and the instrumentation for the flow measurements. A comparison of the 3-hole and 5-hole probe measurements is presented. The experimental results are compared with calculated results taken from a two-dimensional off-design calculation program with standard loss models. By means of the measured static-pressure rise at the casing wall and the total pressure distributions downstream of the rotor rows, a modification of the loss modeling was performed. The calculated flow field is compared to the results of the 3-hole and 5- hole probe measurements in terms of radial distributions for flow angle, Mach number and total pressure.

1. INTRODUCTION

Detailed experimental investigations were carried out at the Siemens test-facility in Berlin to validate and develop further the compressor design of the Model V84.3 gas turbine and to generate a comprehensive data base for the verification of the flow calculation programs devised to predict the flow field in single cascades, as well as in multistage axialflow compressors.

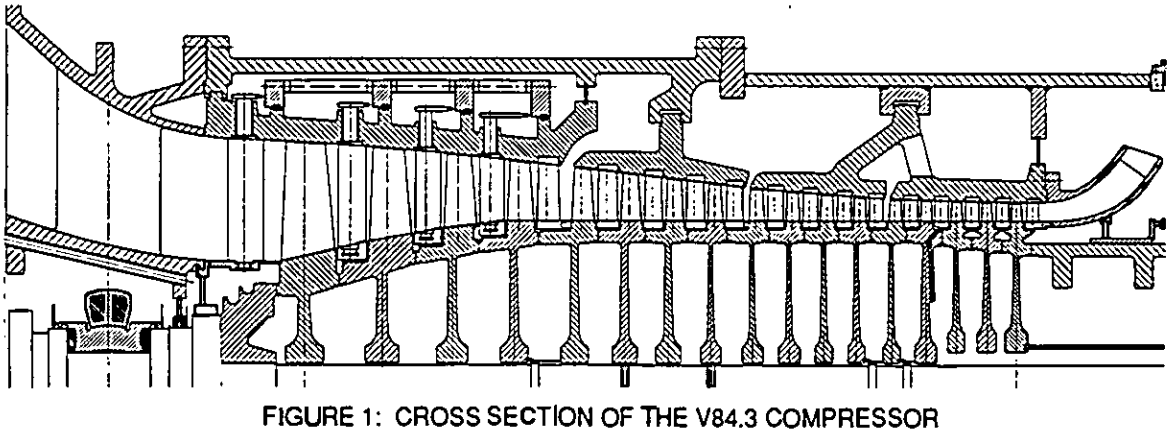

FIGURE 1: CROSS SECTION OF THE V84.3 COMPRESSOR

Presented at the International Gas Turbine and Aeroengine Congress and Exposition
The Hague, Netherlands — June 13–16, 1994

Figure 1 shows a cross-section of the 17-stage axial-flow compressor designed for a rotational speed of 3600 rpm, a mass flow of about 420 kg/s and a pressure ratio of 16:1. High tip speeds of the first and second rotor blades result in relative rotor inlet Mach numbers of about 0.9. The profiles are of supercritical design to ensure low losses and high pressure ratios in these stages. The first three stages are equipped with variable-pitch vanes in addition to the variable inlet guide vanes to improve the part-load efficiency. The compressor has 3 bleeds, located upstream of the blade rows 5, 10 and 14 to avoid surge during start-up and shut-down . The compressor design is described in some more detail by Becker and Ziegner (1988).

Figure 2 illustrates the types and location of the instrumentation used for the compressor measurements in the factory test facility. In addition to the probe measurements and the wall-pressure measurements reflecting the flow field through the entire compressor, the first-stage vane was investigated in some greater detail. First results of these measurements have already been presented by Janssen et al. (1993) and Bohn et al. (1994).

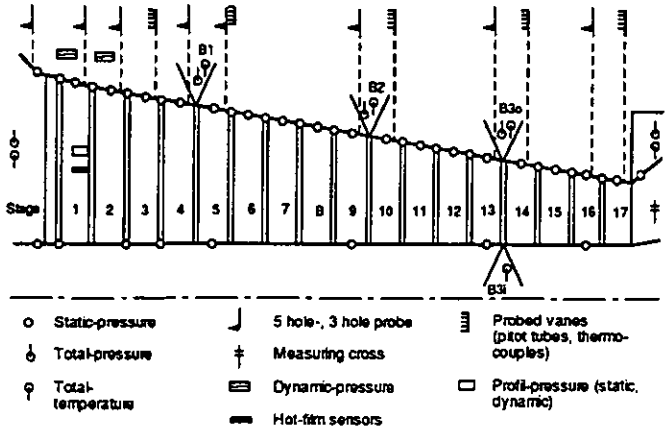

FIGURE 2: INSTRUMENTATION FOR FLOW MEASUREMENTS

All measurements serve as a data base for the verification of computational codes and hence serve as a basic means to develop further the compressor.

2. THE MODEL V84.3 SHOP TESTS

A series of comprehensive tests were conducted from April 1992 through February 1993, on the new-generation Model V84.3 gas turbine for 60 Hz power generation. Siemens possesses the unique capability in its Berlin factory to test large heavy-duty gas turbines at full load, in case of the Model V84.3 machine up to 150 MW. The test facility is described by Deblon (1978). The layout of the test bed is shown in Fig. 3.

The shaft power output of the gas turbine is converted into thermal energy by a water brake rigidly coupled via a torque-measuring shaft. The heat generated is dissipated by three cooling towers. On account of this dynamometer, the operation of the gas turbine can be tested over a wider load and speed range than is possible in power plants.

3. INSTRUMENTATION

The radial distribution of the flow field was measured over the entire span using two methods:

- probed vanes to measure the distribution of total pressure and temperature near the leading edge, and

- traversing 5-hole and 3-hole probes to measure the radial distribution of the velocity vector

Both methods average the flow quantities over several seconds, the time-limiting components being the pneumatic transmission lines. The pressures were measured with Rosemount capacitive pressure transducers, the temperatures with Type K thermo-couples. The A/D conversion was carried out by HP3852A data acquisition/control units. The conversion to engineering units was carried out by the computers as described below.

Additionally, pressure taps at the casing in all the compressor stages and at the hub in selected stages were applied to measure the static pressures at the endwalls and the pressure rise along the compressor.

Probed vanes

Radial distributions of total pressure and total temperature were acquired on the 3rd, 5th, 10th, 14th and 17th-stage compressor vanes. The pressure was measured using pitot tubes at nine radial locations simultaneously.

The conversion to engineering units was carried out by the HP3852A scanners' own processors. The data were acquired by the HP 9000-series thermodynamic data acquisition computer via an IEEE488 interface bus.

5-hole probes

The radial distributions of the flow vector are generated from 5-hole probe measurements at radial locations between approximately 5% and 95% of blade height. Radial traverses are located between vanes, a short distance upstream of the leading edges at approximately half-pitch location.

Figure 4 shows a 5-hole probe, a thermocouple probe and the 3-hole probe discussed below. The pressures were measured with Rosemount capacitive pressure transducers, the temperatures with Type K thermocouples. The A/D conversion was carried out by HP3852A scanners. A data acquisition and control program running on a PC connected with an IEEE488 interface bus carried out the conversion to engineering units and controlled the probe traversing device.

Radial traverses and the rotation of the probe around the shaft

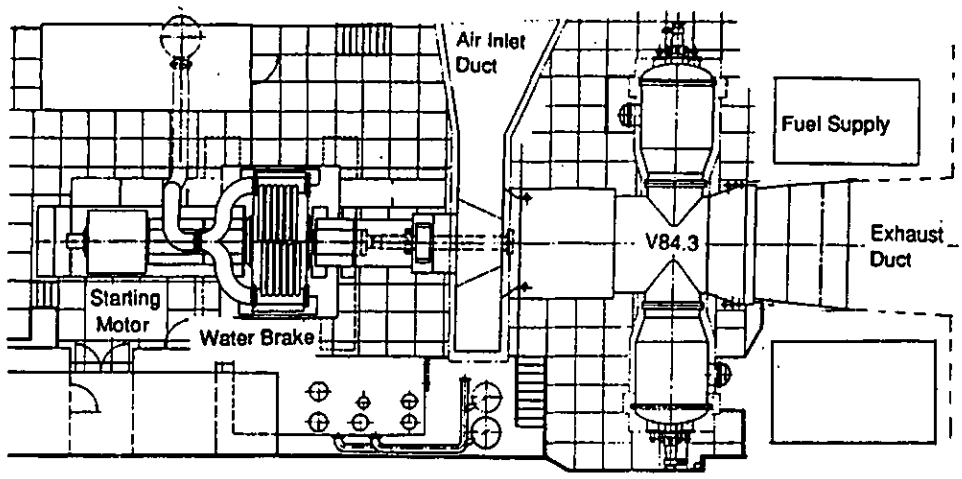

FIGURE 3: ARRANGEMENT OF THE TEST BED

axis were achieved with a probe-traversing device bolted to a flange on the outer compressor casing. The yaw angle is obtained by balancing the pressure across the wedge of the 5-hole probe. The feed-back loop for the yaw angle is embedded in the data acquisition software run on the PC.

The probe-traversing devices were controlled via an IEEE488/RS232 converter by Madis amplifiers and DC servo-motors. The probe shafts were sealed against the leakage of compressor air with a PTFE-based packing. In the 9th through the 16th stage, cooled flanges were used to prevent overheating of the probe-traversing device.

The pitch angle and the magnitude of the flow vector were calculated from the pressure signals of the 5-hole probe. The yaw-angle position of the probe is set such that the residual pressure difference at the wedge falls below a certain threshold. Below this threshold, the yaw angle is further corrected based on calibration data.

Miniature 3-hole probes

Specially designed 3-hole probes were applied to investigate the distributions of velocity and angle near the hub and the casing (Fig. 4). The aim of this newly developed type of probe was to minimize the disturbance of the flow at measuring positions close to the wall. The small size of the probe head (0.7 mm in height, 1.3 mm in width) only allowed a parallel alignment of the three measuring holes. The first part of the shaft has a diameter of 2.5 mm. In combination with a probe-specific calibrating method, the stagnation pressure, the flow angle, and the Mach number could be calculated from the measured data.

These probes were inserted through the same big casing holes (12 and 16 mm in diameter) as the other measuring probes. A plug matching the flow-passage contour was inserted in order to avoid disturbances of the boundary layer near the casing due

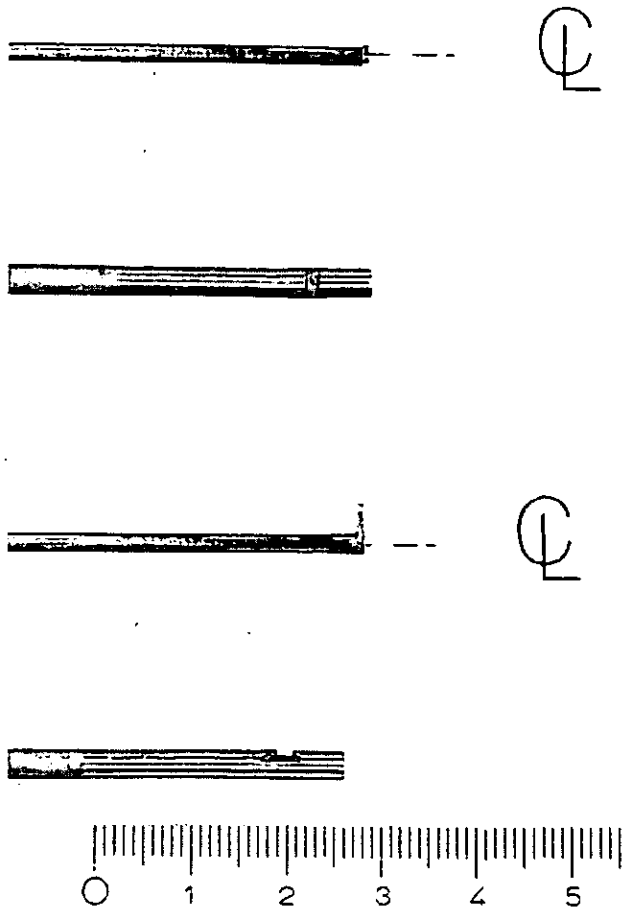

FIGURE 4: COMPARISON OF THE PROBES FOR FLOW MEASUREMENTS, 3-HOLE (TOP), 5-HOLE (BOTTOM)

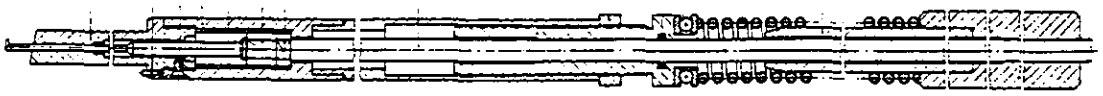

FIGURE 5: MOUNTING LANCE FOR CASING WALL BOUNDARY LAYER MEASUREMENTS

to leakage flow into these holes (Fig. 5). In this way the thin probe shaft was enclosed by this adapter. A special mounting lance had been constructed as a part of the probe to position the plugs in the inner casing without having to dismantle the outer casing.

The uncertainty analysis for steady flow conditions revealed the results summarized in theTable 1.

Stage	Total pressure/ reference pressure (-)	Flow angle (degree)	Mach number (-)
2	$\pm 3{,}2 \cdot 10^{-4}$	± 0.5	± 0.005
9	$\pm 1{,}3 \cdot 10^{-3}$	± 0.5	± 0.005
16	$\pm 1{,}3 \cdot 10^{-3}$	± 0.5	± 0.005

TABLE 1: 90% UNCERTAINTY INTERVALS OF PROBE MEASUREMENTS (3-, 5-HOLE)

4. COMPUTATIONAL METHOD

The calculations regarding both design and off-design performance of the compressor were carried out by means of a streamline-curvature code. The code is based on the classical duct-flow method developed by DYNATECH. The code has been continuously improved in regard to convergence behavior and loss modeling.

The computational method incorporates correlations for several loss mechanisms, such as:

- reference incidence profile losses (minimum losses)
- profile losses caused by off-design incidence
- shock losses
- endwall losses

The endwall losses include the 3D flow effects leading to increased loss rates in the near-wall regions, in particular

- tip-clearance losses
- losses caused by secondary-flow effects and
- endwall boundary-layer losses

The endwall losses are modeled by a decrease of total pressure resulting in low meridional velocities near the walls. As a result, a streamline deflection and consequently also a blockage effect were incorporated into the computational approach without performing any additional endwall boundary-layer calculation.

However, 3D flow effects are known to lead to additional deviation in flow angle, as has been reported by Roberts et al. (1986). Additional deviation was neglected in the calculation presented in this paper. The resulting flow effects, however, were modeled by an increased amount of endwall losses.

5. EXPERIMENTAL RESULTS

Comparison of the Pneumatic Probe measurements

The radial distributions of the flow field are measured in the stator inlet plane of three compressor stages as shown in Figs. 6 through 8. Mach numbers are based on the local static pressure obtained via the probe calibration. Solely the flow regions close to the end walls of the compressor were investigated with the miniature 3-hole probes. The required minimum distance to the wall could be reduced to only 0.8 mm due to the particular design discussed above. Thus, the flow measurements could be extended to those areas of primary interest with respect to loss reduction, blade-shape optimization and the determination of the stable operating range.The 5-hole probes were applied in the core flow. In a small region of about 5 mm the measuring ranges of both types overlapped. Measurements were taken for two no-load operating points (closed vanes --> approximately 75% mass flow and open vanes --> 100% mass flow).

The measured data upstream of the 2nd-stage stator are shown in Fig. 6. The variation of the mass flow rate (variable vane setting) caused changes in flow angle and Mach number. A very good agreement between 5-hole and 3-hole results for both operating points was found for total pressure and flow angle. The deviations in Mach number between 3-hole and 5-hole probe were quite high, because in this case incompressible calibration data were used for the 5-hole probe.

Figure 7 represent the flow distributions upstream of the 9th-stage stator. The deviations in the results of both measuring techniques became clearly visible. The differences in angle reach up to 5 degrees and in total pressure up to 20% independently of the operating point. An explanation of the discrepancies in flow angle is discussed in detail in section 6

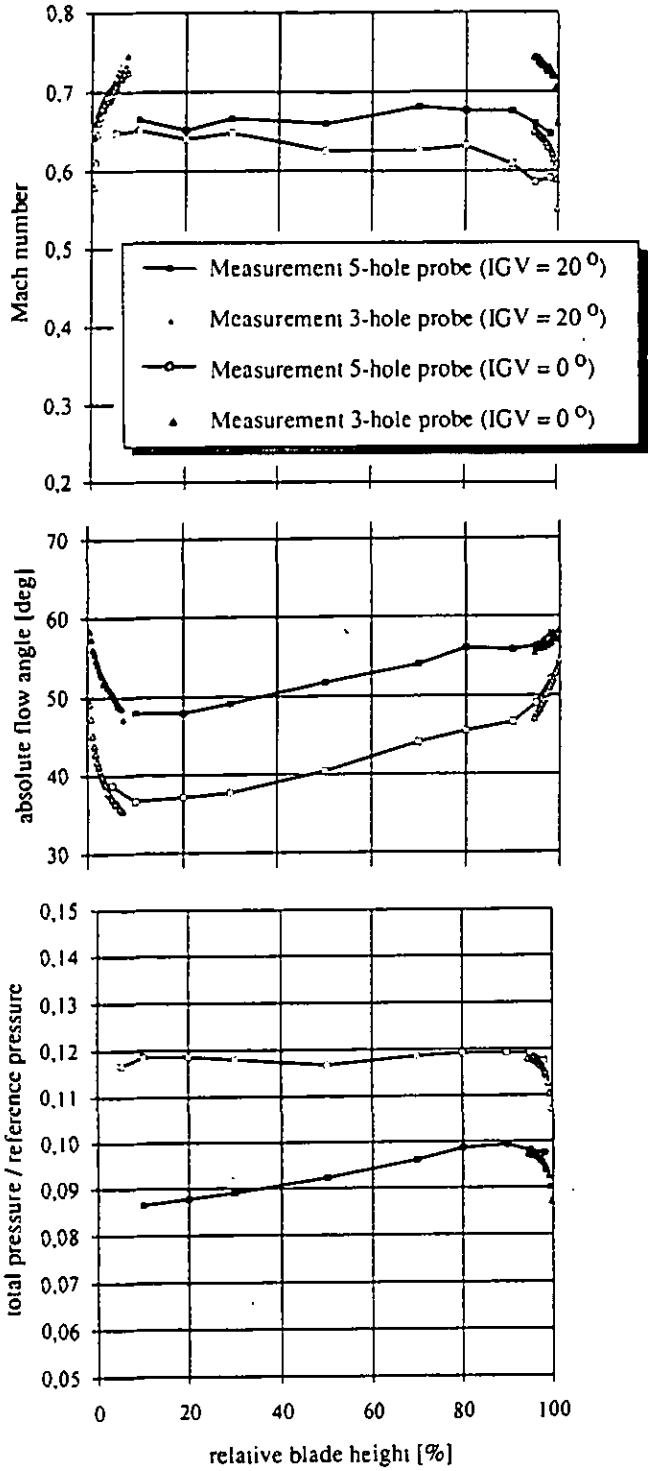

FIGURE 6: 3-HOLE AND 5-HOLE MEASUREMENTS UPSTREAM OF STATOR 2

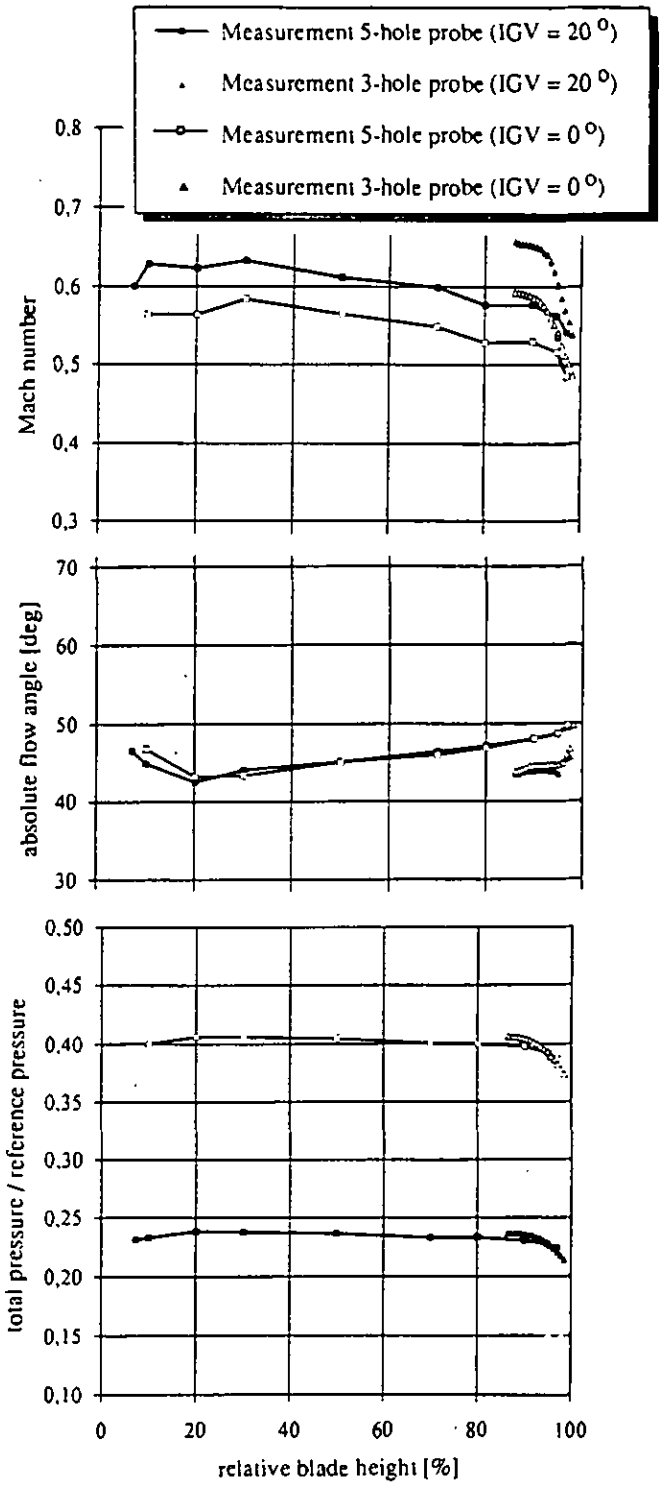

FIGURE 7: 3-HOLE AND 5-HOLE MEASUREMENTS UPSTREAM OF STATOR 9

below.

In the small flow channels the gradients of the flow profiles near the wall measured with the 3-hole probe were found to be steeper than the ones measured with the 5-hole probe. The deviations in Mach number were as high as the ones measured in the 2nd stage.

In the 16th stage the agreement of the Mach numbers for no-load with closed vanes is very good, whereas for no-load with open vanes differences of about 10% could be observed (Fig. 8 top). The differences between results for total pressure and flow angle are within an acceptable range (Fig. 8 bottom, middle). Variations are due to the measuring uncertainty. The casing boundary layer can be found in a region of about 85 to 100% of blade height, nearly independent of the operating point.

The increasing deviation between 5-hole and 3-hole results from the first to the last stage was striking. This phenomenon was found to be caused by the unsteady flow effects. The influence of the fluctuating flow vector on the steady measuring data depends on the probe-head geometry. An investigation of the dynamic behavior of different probe-head geometries was started with the goal of providing a correction method for the measured data. Another reason for the increase of the deviations with stage number is the measuring location. The measuring location of both types of probe is not exactly the same. Due to the probe-head size the pressure taps of the 3-hole probes are positioned about 2 to 3 mm upstream of those of the 5-hole probes, which has a strong influence with smaller chord lengths, hence with increasing stage number. Naturally, Reynolds-number effects also affect the results. But in the case of the flow angle measurements the probes were aligned with the flow instead of calculating the flow angle from a calibration map. Thus, the flow angle is independent of the Reynolds number.

The shape of the flow-parameter distributions in all stages was determined with the same accuracy for both measuring techniques. The total pressure distribution upstream of the 5th-stage vanes was measured by 3-hole probe, 5-hole probe and total-pressure tappings on the vane. A comparison of these distributions, as presented by Janssen et al. (1993), shows very good matching and verifies the total- pressure measurements by 3-hole and 5-hole probes for the front stages of the compressor. Due to the smaller probe-head dimensions and the high density of measuring points the side-wall boundary-layer regions were represented in greater detail by the 3-hole probes.

The Mach numbers and total pressures in the endwall regions decreased due to the boundary-layer losses near hub and casing. A sharp increase of the flow angles could be observed in the same regions .

The growth of the casing-wall boundary layer throughout the compressor is illustrated in Fig. 9. The increase of the relative boundary-layer displacement-thickness was influenced by the contour of the flow channel and the bleeds behind the 4th, 9th and 13th stage.

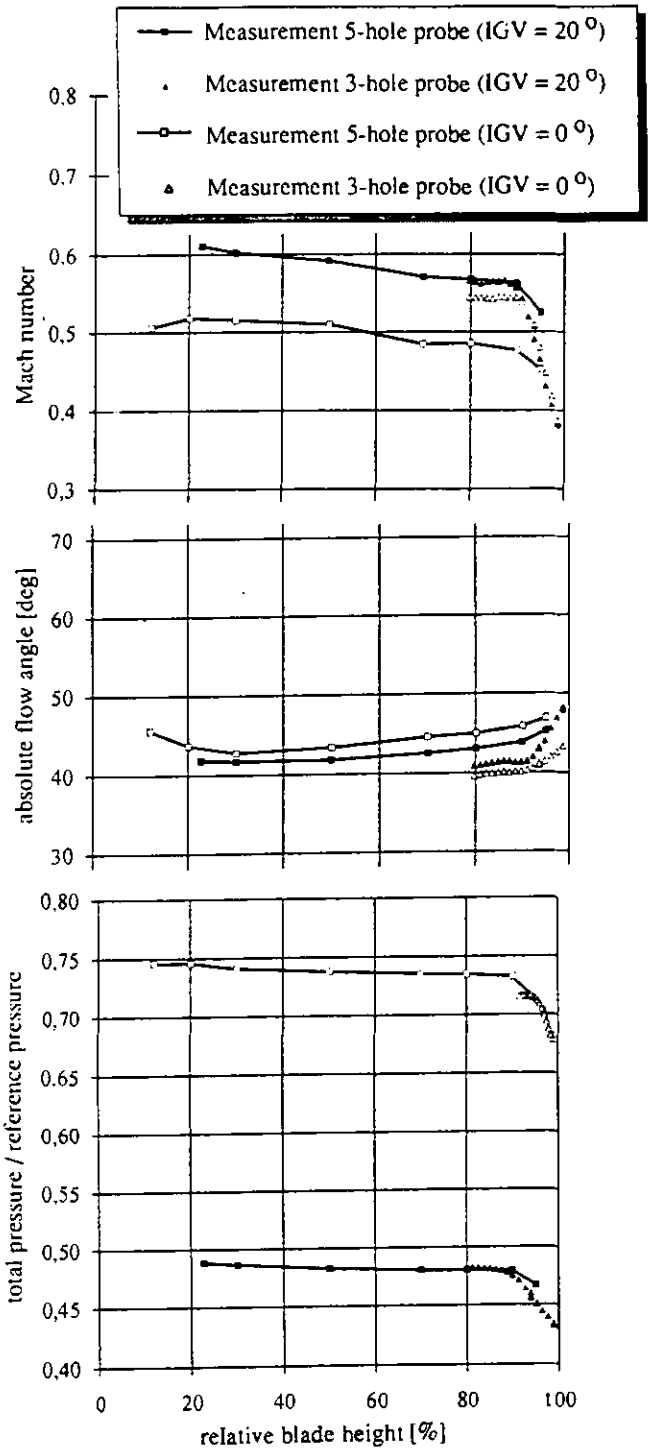

FIGURE 8: 3-HOLE AND 5-HOLE MEASUREMENTS UPSTREAM OF STATOR 16

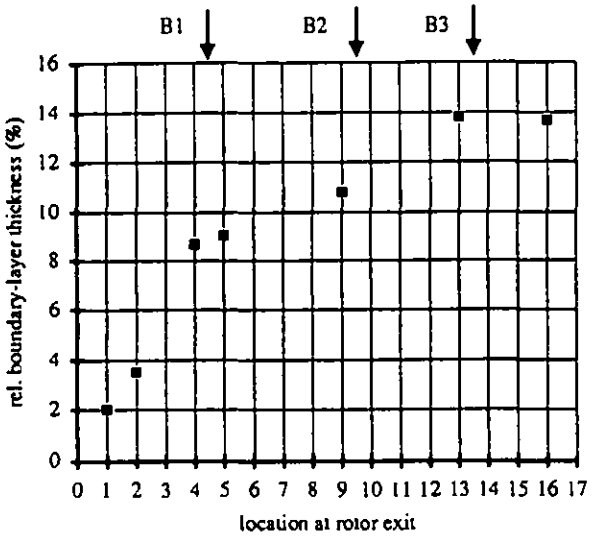

FIGURE 9: DEVELOPMENT OF CASING WALL BOUNDARY LAYER

6. ESTIMATION OF MEASURING ERROR FOR THE TWO PROBE TYPES

The comparison of the measuring results demonstrates the increasing deviation of the flow angle values between both probe types with increasing stage number. This effect is attributed to the influence of unsteadiness due to the rotor wake on the mean value of the pneumatic measurement.

Several investigations on this problem were carried out in the past. The influence of different transmission lines between measuring location and transducer was described by Tijdeman and Bergh (1972) and Klonowicz (1985). Another error is caused by unsteady flow effects occuring at the probe head. This phenomenon applies to the probe measurements discussed

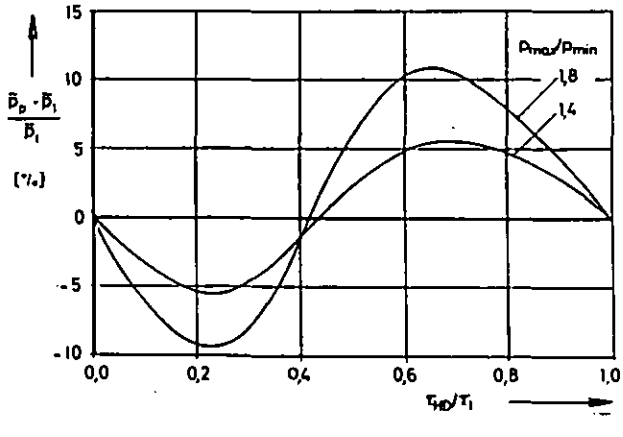

FIGURE 10: MEASURING ERROR AS A FUNCTION OF TIME RATIO t_{HD}/t

in chapter 5. Weyer (1973) researched the influence of several parameters for different flow and measuring conditions.

The essence of his investigations is given in Fig. 10. The x-axis is a dimensionless time scale reflecting the circumferential extension of the wake versus the spacing of the rotor row upstream of the measuring plane. The extrem values are zero, which means that there is no wake at all, and one, indicating that the wake extends over the entire spacing. In this case the wake and the free stream are becoming identical. The y-axis reflects the measuring error, expressed as the difference between the time averaged pressure a pressure taping would measure if the probe were aligned with the flow vector at any time and the measured time averaged pressure, nondimensionalized by the measured time averaged pressure. The dependence of measuring error from the circumferential extension of the wake is given for two pressure ratios (pmax/pmin, where pmax (pmin) is the maximum (minimum) pressure detected by the pressure taping). The pressure ratio is not only a measure for the strength of the wake but also dependent on the location and orientation of the pressure hole relativE to the flow vector. In case of the two probe types used for the measurements in the V84.3 compressor the location of

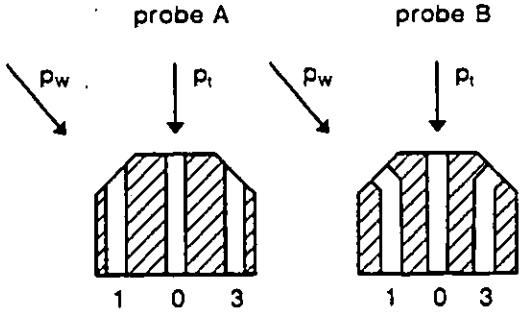

FIGURE 11: NOMENCLATURE FOR THE COMPARISON OF PROBE A/B

the pressure holes is almost the same, the orientation however is quite different, as can be seen in Fig. 11.

To show how this affects the pressure ratio p_{max}/p_{min} (and, as a result, also the measured flow angle) we will refer to pressure tap 1 and 3 of both probes. Assume that the nondimensionalized total pressure of the undisturbed flow is 2 and the nondimensionalized static pressure is 1. Furthermore we assume that the rotor wake extends over 20% of the spacing, that the static pressure is constant along the circumference and that the pressure measured with a pressure tap oriented in such way that the centerline is 45 ° declined to the flow direction is approximately 75% of the total pressure. With these assumptions the pressure ratios and time ratios are estimated. Regarding the velocity triangles for the axial plane upstream of the stator-row of stage 16, the absolute velocity in the wake is approximately equal to the absolute velocity of the undisturbed

flow, what means that the difference in total pressure in the wake and in the undisturbed flow is negligible. The result for the above described example is summarized in Table 2.

	probe A hole 1	hole 3	probe B hole 1	hole 3
p_{max}/p_{min}	$p_t/0.75*p_t$	p_t/p_s	$p_{tw}/0.75*p_t$	$0.75*p_t/p_s$
	1.33	2	1.33	1.5
τ_{HW}/τ	0.8	0.8	0.2	0.8

TABLE 2: PARAMETERS FOR PROBE A/B (EXAMPLE)

The strongly simplified situation discussed above reveals two main conclusions, which can be adressed to the real flow situation as well. First, the measuring error for the pressure taps one and three is different. This results in an erronuous alignment of the probe and hence in a wrong determination of the flow angle. Second, the magnitude of measuring error is dependent on the orientation of the pressure tapings. This yields a difference in measuring error for the two probe types.

To get more information about the magnitude and the difference of measuring error of both probe types and to derive a correction method for the probe measurements in unsteady flows in terms of a flow angle correction, theoretical and experimental investigations have to be continued.

7. COMPARISON OF EXPERIMENTAL RESULTS WITH CALCULATIONS

Figure 12 shows the static pressure rise at the casing wall during no-load and close to base-load opertion. As expected, the influence of increasing backpressure was visible only in the rear section of the compressor. The comparison with calculated results showed good agreement and confirmed the good aerodynamic matching of the stages, as well as the validity of

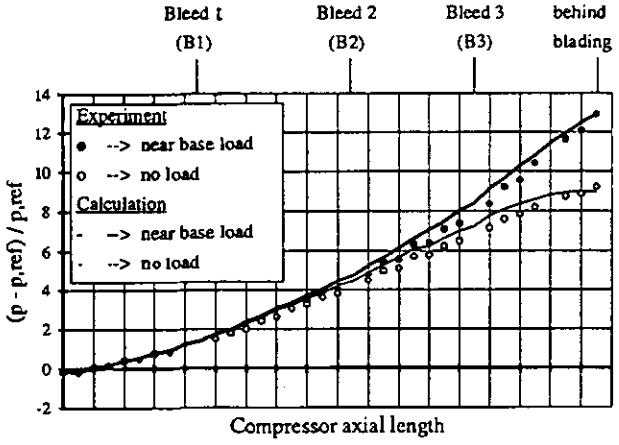

FIGURE 12: STATIC PRESSURE DEVELOPMENT AT THE CASING WALL

the design tools.

A no-load operating point at design speed and design guide-vane setting was selected (maximum mass-flow condition) to compare the probe measurements and calculations. For this comparison a low-pressure stage (No. 2), an intermediate-pressure stage (No. 9) and a high-pressure stage (No. 16) were chosen.

Low-pressure stage

The distribution of Mach number, absolute flow angle and total pressure upstream of stator vane 2 are shown in Figs. 13 versus relative blade height (0% --> hub, 100% --> casing).

The 5-hole probe measurements, as well as the computations, demonstrated that the Mach number decreased slightly towards the casing (Fig.13 top). However, the measured distribution was lower than predicted by computation. This can be explained by the calibration procedure of this probe which was performed only at incompressible flow conditions. The agreement of the calculation and the results obtained by the boundary-layer probe were quite satisfactory. Especially in the end-wall regions, the Mach number decrease due to loss-accumulation was simulated quite well.

The absolute flow angle versus the meridional direction is shown in Fig. 13 (middle). The reference incidence flow angle of the stator blade is represented by the dotted line. In this case, the probe measurements uniformly indicated a negative incidence of about 3 degrees occuring in the core region. The matching of the results obtained by boundary-layer probe and 5-hole probe was also satisfactory at this location. The calculations, however, predicted a positive incidence angle of about 3 degrees at the stator inlet. This deviation from the measured value is attributed to the poor approximation of the off-design operating behavior (loss and deflection characteristics) of the upstream rotor in the streamline-curvature code. However, the predicted slope of the absolute flow angle was again in close agreement with the measurements.

The distribution of stagnation pressure is given in Fig. 13 (bottom). An increasing deviation from the measured values was observed in the outer flow region. This phenomenon is attributed to the rotor Mach numbers being in excess of the design value, resulting in an increased level of shock losses.

Intermediate stage

Mach number, absolute flow angle, and total pressure for the intermediate stage are plotted in Figures 14.

Compared to the low-pressure stage, the Mach number decreased due to the temperature rise. In this case the calculated distribution was in close agreement with the measurements performed by means of the 5-hole probe (Fig. 14 top). The significant decrease at the casing detected by the boundary-layer probe was not fully simulated by the computations. In this context it must be kept in mind that the computation was based on the inviscid equations regarding conservation of momentum and energy.

Thus a positive value of the meridional flow velocity is required at all locations within an axial gap, including the wall streamlines. This implies that the end-wall losses have to be limited to a certain value in order to avoid a failure of the computing technique for off-design flow conditions.

In contrast to the low-pressure stage discussed above, the predicted flow angle was in close agreement with the 5-hole probe measurements for stator vane 9 (Fig. 14 middle). The distributions of flow angle and Mach number show that the aerodynamical loading was also predicted in a correct manner. The increase in absolute flow angle close to the casing wall was qualitatively reproduced by the computation. The steep rise of the flow angle directly at the casing was not exactly simulated by the theory due to the aforementioned reasons.

The total-pressure rise derived from the calculation was higher than the values found by both 5-hole and boundary-layer measurements (Fig. 14 bottom). The deficiency is thought to be caused by the absence of a spanwise mixing model. Thus the energy and momentum transport from one streamline to another is completely suppressed. In fact, this leads to higher total-pressure values within the core region because a transport of fluid with lower total pressure towards the mid-section is computationally impossible. The implementation of radial mixing would allow higher end-wall losses to be prescribed and hence result in a decrease of stagnation pressure level.

High-pressure stage

The phenomena already observed in the intermediate stage become even more obvious in the rear stage. The Mach-number distribution (Fig. 15 top) again shows an excellent agreement with the flow measurements carried out by the 5-hole probe. The deviation of the boundary-layer probe measurements were discussed in detail in Section 4 above. The mass-flow-averaged Mach number reveals a further decrease caused by temperature influence.

The spanwise distribution of the absolute flow angle still reveals a negative incidence of 4 to 7 degrees at midspan (Fig. 15 middle). Thus, there is a sufficiently large surge margin which is required for maximum loading of the compressor. Furthermore, the additional surge margin required for unfavorable operating conditions of the gas turbine is available. The slope measured at the casing by means of the 3-hole probe was in close agreement with the calculation at this location, whereas the absolute value again differed significantly.

However, a discrepancy occurred in regard to the steeply decreasing Mach number near the casing and the moderate increase of the absolute flow angle. Obviously, the gradient of the flow angle was already diminished at the measuring section. This is very likely caused by unfavorable design constraints leading to the necessity that the probe be placed within the inlet section of the stator vane at about 15% of the chord length.

Comparing the measured total pressure upstream of stator vane 16 to the flow angle, it becomes evident that there are still high-loss regions directly at the casing, leading to the observed drop in stagnation pressure (Fig. 15 bottom). Again, the absolute value of total-pressure increase was overestimated by the computation due to the radial-mixing effects being neglected.

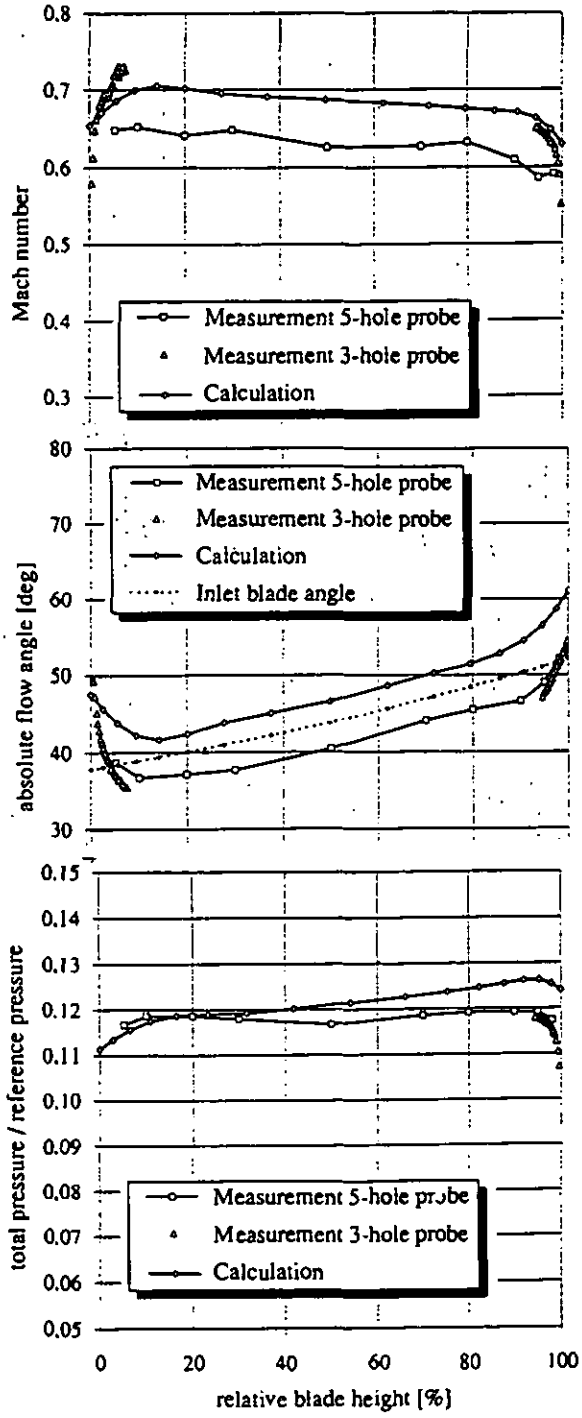

FIGURE13: COMPARISON OF CALCULATED AND MEASURED RESULTS FOR THE FLOW FIELD UPSTREAM OF STATOR 2

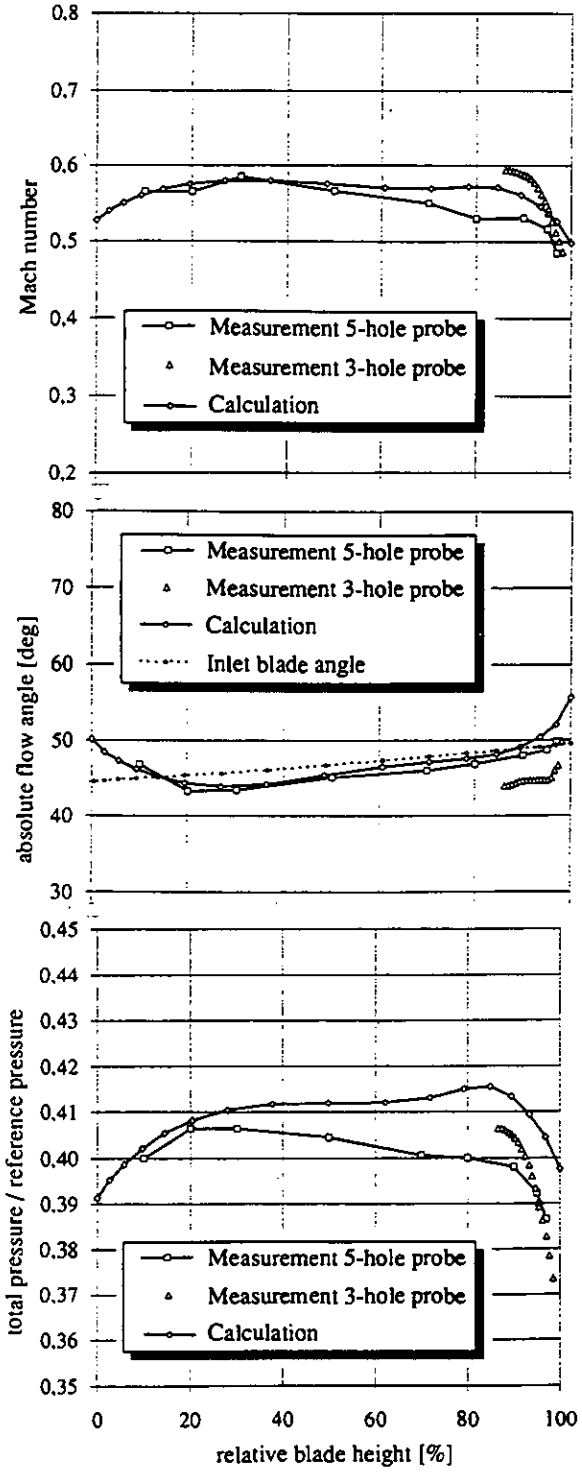

FIGURE14: COMPARISON OF CALCULATED AND MEASURED RESULTS FOR THE FLOW FIELD UPSTREAM OF STATOR 9

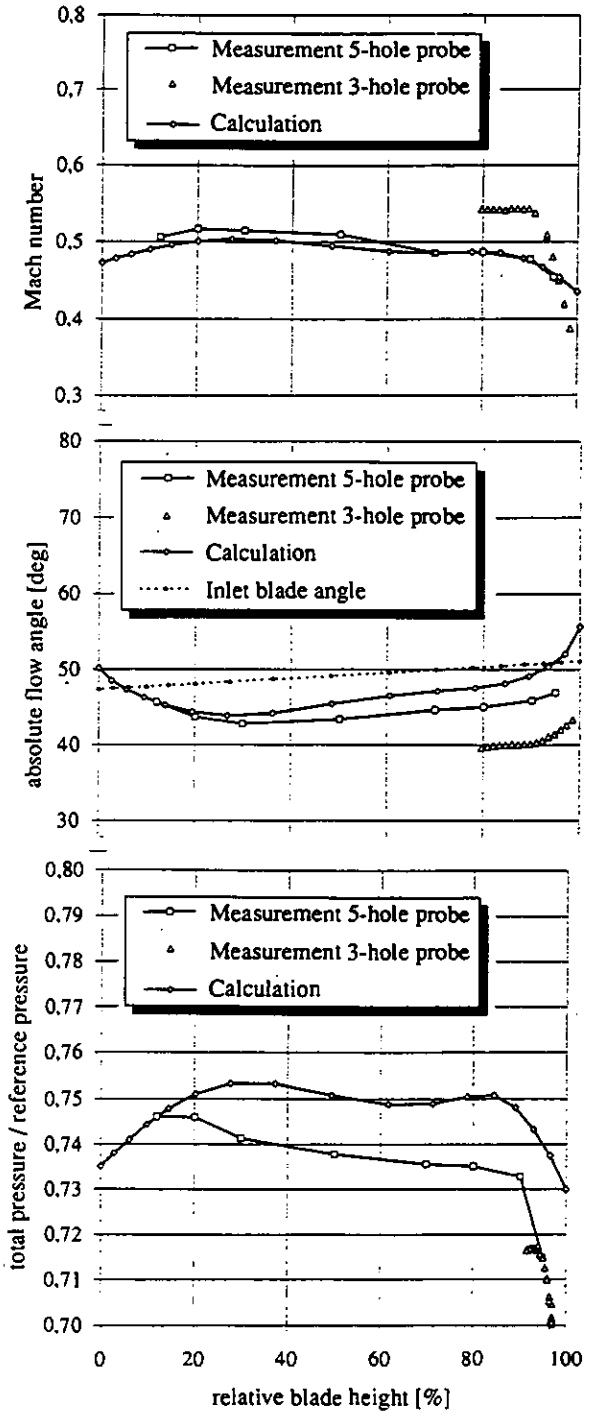

FIGURE15: COMPARISON OF CALCULATED AND MEASURED RESULTS FOR THE FLOW FIELD UPSTREAM OF STATOR 16

8. CONCLUSION

Conventional (5-hole probe, probed vanes, static wall pressure), as well as new measurement techniques (3-hole boundary-layer probe) were adopted to investigate the flow field in the axial-flow compressor of the Model V84.3 gas turbine.

The comparison of the 3-hole and 5-hole probe results for the front stages (2nd stage) showed good agreement for all flow quantities considered. However, with higher stage number the deviations in flow angle and Mach number increased. It is assumed that these phenomena are mainly caused by

- unsteady flow-effects, which strongly depend on the geometry of the probe head
- the axial position of the pressure taps, which is different for the 3-hole and the 5-hole probes and
- Reynolds-number effects,

which affect the pressure and as a result the Mach-number measurements. Preliminary investigations for a single stage research compressor with IGV conducted at the turbomachinery laboratory of the Technical University Aachen verified the assumption concerning the effect of unsteady flow-effects. To correct for the different axial positions of the 3-hole and 5-hole probe heads 3D flow calculations will be performed. Rough estimates have already shown that both corrections result in improved agreement. Reynolds-number effects are thought to play a rather negligible role and have not yet been investigated closer.

The modification of standard loss-models used in the streamline-curvature code by defining additional losses to match the measured total-pressure distributions does not in all cases lead to satisfactory results. The reasons for these sometimes large deviations are manifold. A considerable improvement is anticipated by the insertion of a calibrated mixing model and a correlation for additional deviation derived from the flow-field measurements.

The present exploration of the experimental data base generated from Model V84.3 shop tests confirmed the compressor design of Siemens' new-generation gas turbines. Furthermore, it validates the availability of conventional as well as new measurement techniques for the multistage environment of industrial compressors. Improvements and corrections of the probe measurements and the numerical code were derived from the test data and will be further investigated by additional measurements and 3D calculations.

Based on the detailed measurements presented above, further improvements in the design of Siemens' axial-flow compressors will be introduced. The paper shows the development and implementation of detailed aerodynamic measurements which are a prerequisite for further refinement of turbomachinary design. The availability of the Siemens' full-load test facility for such measurements lends a unique strength to securing optimum performance of its gas turbines.

ACKNOWLEDGEMENT

This work is part of the AG TURBO research program, a cooperative effort between Industry, Universities and National Research Centers, financially supported by the German Ministry of Research and Technology (BMFT).

REFERENCES

B. Becker, M. Ziegner, "The New Siemens/KWU Model V64.3 Gas Turbine", MTZ Motortechnische Zeitschrift 49 (1988) 6, pp. 233-240.

D. Bohn, Th. Schnittfeld, M. Janssen, "Stationäre und instationäre Belastungen von Verdichter- und Turbinenleitschaufeln in einer Hochtemperaturgasturbine vom Typ V84.3", to be published at VDI - GET - Fachtagung, March 1994, Aachen, Germany.

B. Deblon, "Full Load Tests of the 80 MW Gas Turbine V93.2 using a Water Brake", ASME 78-GT-68, 1978.

M. Janssen, J. Seume, H. Hönen, R. Lösch-Schloms, H. E. Gallus, "Flow Field Analysis of the Axial Compressor of the Siemens V84.3", CIMAC 1993, GT-27.

W. Klonowicz, "Measurements of the Time Averaged Fluctuating Gas Pressure within Thin Tubes", Ph.D thesis, Universtiy of Strathclyde, 1985.

W. B. Roberts, G. K. Serovy, D. M. Sandercock, "Modeling the 3-D Flow Effects on Deviation Angle for Axial Compressor Middle Stages", Journal of Eng. for Gas Turbines and Power, Vol. 108, 1986.

H. Tijdeman, H. Bergh, "The Influence of the Main Flow on the Transfer Function of Tube-Transducer Systems used for Unsteady Pressure Measurements", NLR MP 72023U.